Influence of material's yield strength on the kinematic hardening of steels

Article *in* Steel Research International · January 2012

CITATIONS
2

READS
55

4 authors:

Joseba Mendiguren
Mondragon Unibertsitatea
89 PUBLICATIONS **751** CITATIONS
SEE PROFILE

Lander Galdos
Mondragon Unibertsitatea
113 PUBLICATIONS **826** CITATIONS
SEE PROFILE

Eneko Sáenz de Argandoña
Mondragon Unibertsitatea
88 PUBLICATIONS **642** CITATIONS
SEE PROFILE

Elena Silvestre
Ikergune - Inzu Group
21 PUBLICATIONS **128** CITATIONS
SEE PROFILE

Influence of material's Yield Strength on the Kinematic Hardening of steels

Joseba Mendiguren, Lander Galdos, Eneko Sáenz de Argandoña, Elena Silvestre

(1) Mondragon University – Mechanical and Manufacturing Department – Spain – jmendiguren@mondragon.edu

Abstract. In the last years, and mainly due to the constantly increasing market competitiveness, there has been a trend towards more and more complex geometries, design free structures and new materials with higher ultimate tensile strengths and consequently lower formability properties. Common problems are premature cracks, high springback, excessive distortion of the parts, bad final surface quality, etc. All these changes make numerical simulation an indispensable tool for process development. Nevertheless, the numerical results are directly linked to the material and contact description, being the Baushinger phenomenon in cyclic plasticity an important factor for sheet metal forming simulations in those processes where material is subjected to compression-tension stress states. In the present work, the influence of the yield strength on the mixed hardening model parameters is analysed. Kinematic hardening parameters are obtained for DC04, TRIP700 and MS1200 steels. First, tensile tests are performed using a conventional uniaxial tensile machine. Then, using inverse simulation, the parameters of the mixed Chaboche1990 hardening model are obtained. As a result, the Chaboche1990 mixed hardening parameters are obtained and compared to the materials´ yield strength. Back-Stress Tensor stabilizes later when using high strength steels and thus long range of cycles is needed before reaching the stable state when using AHSS.

Keywords: Metal forming, Baushinger phenomenon, kinematic hardening, Chaboche

1. INTRODUCTION

In the last years, and mainly due to the constantly increasing market competitiveness, there has been a trend towards more and more complex geometries, design free structures and new materials. Moreover these challenges have been attempted trying in parallel to reduce the number of manufacturing steps due to economical reasons. All the previous changes applied to sheet metal forming processes have concluded into a scenario where the deformations that materials are subjected during the manufacturing processes have raised considerably being much closer to their formability limits.

Furthermore, new problems have appeared such as premature cracks, springback problems, excessive distortion of the parts, bad final surface quality, etc. All these changes make numerical simulation an indispensable tool for process development. Nevertheless, the numerical results are directly linked to the material and contact description, being the Baushinger phenomenon in cyclic plasticity an important factor for sheet metal forming simulations [1].

Strain path reversal is quite common in sheet metal forming processes, e.g bending-unbending or deep drawing. In steel characterization the tension-compression test is commonly used to obtain the hardening behaviour of the material [2]. The problem of the sample´s buckling that appears in this kind of test in metal sheets has been differently overcomed, e.g using the bending test instead of the tensile test, using special tools to block the buckling [3]. Due to the buckling problem, the kinematic hardening characterization in metal sheets is still a big challenge.

In this work, experimental tension/compression tests are performed in three different steel sheets using a tooling that avoids the buckling. Then, an elastoplastic model with mixed isotropic/kinematic hardening model is fitted to the experimental results to found the hardening parameters for each steel.

Finally, the obtained results are discussed and the influence of the quasi-static material parameters in the hardening parameters are analysed.

2. MATERIAL MODEL

The behaviour law used in this study is a unidimensional elastoplastic associative behaviour law with mixed hardening. The basic equations which compose the material model are presented in the following lines.

The main hypothesis underlying the small strain theory of plasticity is the decomposition of axial strain:

$$\varepsilon = \varepsilon^e + \varepsilon^p, \tag{1}$$

where ε, is the axial strain , ε^e, is the elastic strain and ε^p, represents the plastic strain.

Following the above definition of the strain, the constitutive law for the axial stress can be presented as:

$$\sigma = E\,\varepsilon^e, \tag{2}$$

where σ, is the axial stress, and E is the material's Young's modulus.

In this unidimensional model with mixed hardening the yield function leads:

$$\Phi(\sigma, X, \sigma_y) = |\sigma - X| - \sigma_y, \tag{3}$$

where Φ, represents the yield function, while X, is the backstress tensor characteristic of the kinematic hardening and σ_y, is the size of the yield surface defined by the isotropic hardening.

The plastic flow rule for this unidimensional elastoplastic formulation can be expressed as:

$$\dot{\varepsilon}^p = \dot{\gamma}\, sign(\sigma), \tag{4}$$

where $\dot{\gamma}$, is the plastic multiplier [4] and $sign(\sigma)$ denotes the signum of the stress, σ .

The Chaboche's mixed hardening model is implemented in this work; the kinematic hardening is introduced by using the Armstrong-Frederick formula [5]:

$$dX = C\, d\varepsilon^p - \alpha\, X\, d\bar{\varepsilon}^p, \tag{5}$$

where C and α, are material constants and $d\bar{\varepsilon}^p$, is the increment of accumulated axial plastic strain $\bar{\varepsilon}^p$, defined as:

$$\bar{\varepsilon}^p \equiv \int_0^t \left|\dot{\varepsilon}^p\right| dt. \tag{6}$$

The yield surface size is represented by:

$$\sigma_y = \sigma_{y0} + R, \tag{7}$$

where σ_{y0}, is the initial yield stress and R, represents the isotropic hardening written as:

$$dR = b\left(Q - R\right) d\bar{\varepsilon}^p, \tag{8}$$

where Q, and b, are material parameters.

3. MATERIALS AND EXPERIMENTAL SETUP

In this study three different steels are analysed, a 1.5 mm thickness DC04 mild steel, a 1.48 mm thickness TRIP700 austenitic steel and a 1.45 mm thickness MS1200 martensitic steels. Figure 1 shows the flow curves of these materials and summary is made in Table 1.

Table 1. Quasi-static properties of the analysed materials.

Material	Yield stress σ_y	Maximum stress σ_r	Elongation A
DC04	193 MPa	420 MPa	35 %
TRIP700	400 MPa	940 MPa	25 %
MS1200	1100 MPa	1380 MPa	3 %

MS1200 steel has the highest yield stress but the lowest elongation. On the other hand, DC04 steel has the lowest yield stress but the greatest elongation. The properties of TRIP700 steel are between DC04 steel and MS1200 steel ones.

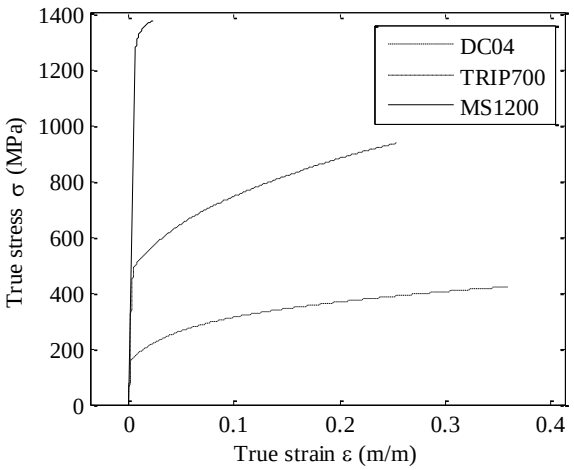

Figure 1. Tensile test behaviour of the analysed materials.

Figure 2 shows the specimen geometry used for the materials´ characterization (tension-compression tests). The calibrated section is 12.5 mm wide and 22.5 mm long. The specimens are cut in a wire electrical discharge machine in order to minimize geometrical deviations.

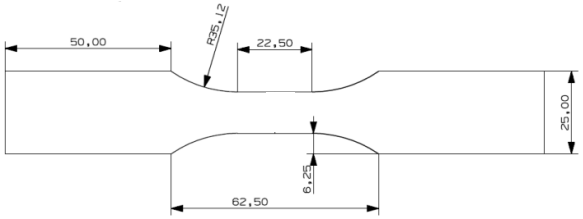

Figure 2: Geometry of the tension-compression specimen.

3.1. Tension/compression tests.

A servo-hydraulic MTS 810 universal fatigue machine is used for tension/compression tests. The strain measurement is performed by 350 Ω strain gages. The specimen is subjected to tension/compression cycles, controlling the servo-hydraulic machine in displacement.

Figure 3 shows the experimental test equipment used to avoid buckling. The specimen is clamped between the two holders and Rhenus Fe 1300 lubricant is used in order to eliminate the influence of friction during the test. One of the holders has a hole where the strain gage is placed.

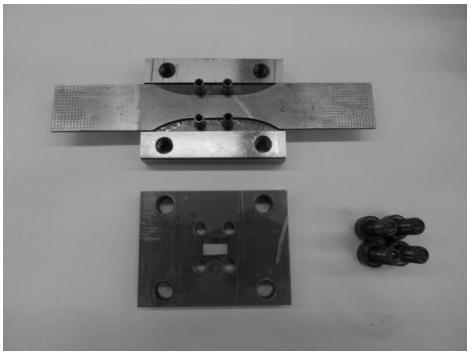

Figure 3. Experimental set up in order to avoid the buckling of the sample.

4. PARAMETER IDENTIFICATION

Figure 4 shows the flowchart of the parameter identification procedure. The procedure starts applying initial values of the hardening parameters. Taking into account the previously presented material model, the stress response of the model to the experimental strain path is calculated using the initial parameters. The Young's modulus of the material is calculated by linear regression following the E111-97 standard.

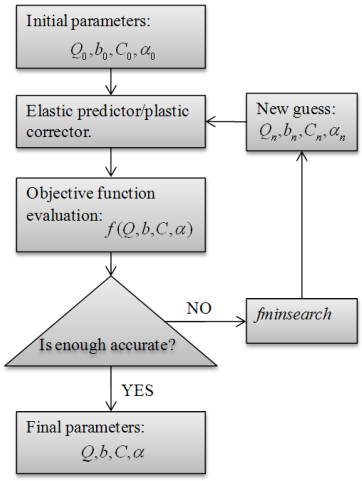

Figure 4. Parameter identification procedure flowchart.

Once the response of the model is obtained using an elastic predictor/plastic corrector algorithm, the objective function is evaluated. The objective function to minimize is:

$$f(Q,b,C,\alpha) = \sum_{i}^{i\max} \left(\sigma(\varepsilon_i) - \sigma_i\right)^2, \tag{9}$$

where, $f(Q,b,C,\alpha)$ represents the objective function, where i, is the index of summation, $i\max$, is the total number of experimental data, $\sigma(\varepsilon_i)$ and σ_i are the stress values of the model and the i-th experimental stress for the i-th experimental strain, ε_i, respectively.

In order to calculate the optimum parameter combination representing the experimental data, the Nelder and Mead minimization method [6], which is implemented in the *fminsearch* function in Matlab® is used. The objective of this algorithm is to propose new parameter combinations until the minimum value of the objective function is reached.

5. RESULTS AND DISSCUSION

In this section the experimental results as well as the numerical response of the model with the optimum parameter combination are shown.

5.1. Experimental and numerical results

Figure 5 shows both, the experimental results and numerical results performed with the optimum parameter combination for the tension/compression test of the DC04 steel.

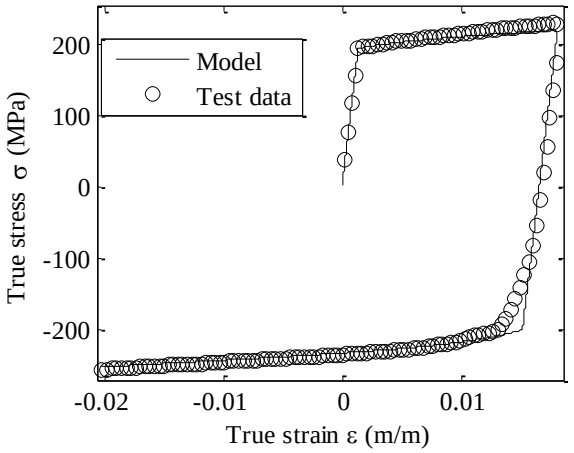

Figure 5. Experimental and numerical results of the DC04 under tension/compression cycle.

In the same way, Figure 6 and Figure 7 show the experimental and numerical results of the tension/compression test of the MS1200 martensitic steel and TRIP700 steel.

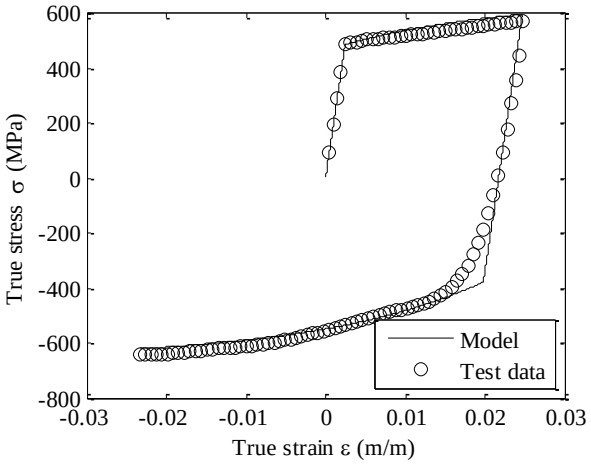

Figure 6. Experimental and numerical results of the TRIP700 under tension/compression cycle.

Table 2 summarises the optimum parameter combination for each material under tension/compression test, obtained with the previously defined identification procedure.

Table 2. Optimum parameter combination for each material under the single tension/compression test.

Material	Q (Pa)	b	C (Pa)	α
DC04	$1.550 \cdot 10^{9}$	0.3532	$4.539 \cdot 10^{9}$	153
TRIP700	$1.963 \cdot 10^{8}$	$9.940 \cdot 10^{-16}$	$8.4842 \cdot 10^{9}$	51.54
MS1200	$1.475 \cdot 10^{8}$	$7.171 \cdot 10^{-14}$	$2.141 \cdot 10^{10}$	18.93

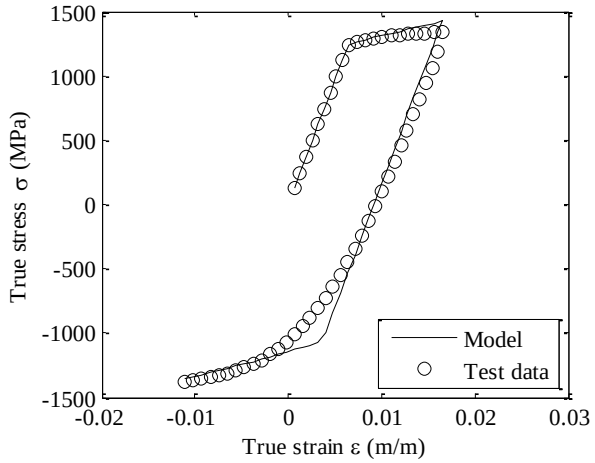

Figure 7. Experimental and numerical results of the MS1200 under tension/compression cycle.

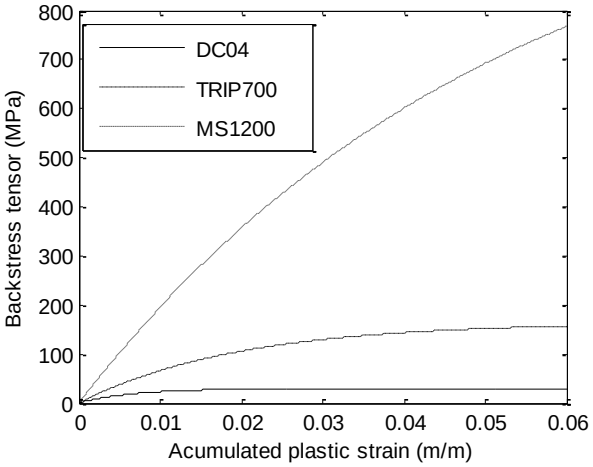

Figure 8. Differences between the kinematic hardening of DC04 and MS1200 steel.

5.2. Discussion

From the fitting of the models shown in Figure 5, Figure 6 and Figure 7 some appreciations can be obtained. Even if the model gets to fit the shape of the experimental data, some limitations can be emphasised. The model seams not to be able to represent the sharp transition from the elastic to the elastoplastic behaviour. Furthermore, in the elastic behaviour at the start of the compression phase, differences are shown between the experimental data and the model's prediction.

The Young's modulus used for the model has been taken from the elastic behaviour at the start of the tension phase. Therefore, these differences can be due to Young's modulus variations under plastic deformation. Some authors have reported this kind of variations in steels [7].

The Chaboche's mixed hardening model has four material parameters. On the one hand, the combination of Q and b parameters gives the evolution of the isotropic hardening. This hardening establishes the evolution of the size of the yield surface. On the other hand, C and α parameters give the displacement of the yield surface without changing its size.

The results exposed in Table 2 for the TRIP and MS steels, show that the preponderant hardening mechanism is the kinematic one. Both have a very low value of b. This low value means that even if the value of Q is important, the change in the yield surface size will be minimum. On the other hand, different behaviour is observed for the DC04, having higger b and Q values.

Figure 8 shows the evolution of the backstress tensor for all the steels in function of the accumulated plastic strain. The DC04 is stabilized around 0.02 of accumulated plastic strain and the TRIP700 seams to reach the stabilized state around 0.06. The MS1200's kinematic behaviour is still growing up at 0.06 of accumulated plastic strain. Therefore a long range of cycles has to be made before reaching the stabilized state with this last material.

6. CONCLUSIONS

The following general conclusions can be pointed out form the present work:

- The model seams not to be able to represent the sharp transition from the elastic to the elastoplastic behaviour.
- The preponderant hardening mechanism is the kinematic hardening for the TRIP700 and the MS1200 steels.
- Back-Stress Tensor stabilizes later when using high strength steels.

7. REFERENCES

[1] B.K.Chun, J.T. Jinn, J.K. Leers: Modeling the Bauschinger effect for sheet metals, part I: Theory, Int J Plasticity 18 (2002), 571-595.

[2] L. Madej , K. Muszka, K. Perzynski, J. Majta, M. Pietrzyk: Computer aided development of the levelling technology for flat products, CIRP Annals - Manufacturing Technology (2011), 291–294.

[3] P.A. Eggertsen, K. Mattiasson: On the identification of kinematic hardening material parameters for accurate springback predictions, International Journal of Material Forming, 4 (2011), 103-120.

[4] E.A. de Souza, D. Peric, D.R.J. Owen: Computational methods for plasticity. Theory and applications, Wiley, UK(2008), 140-190.

[5] J. Lemaitre, J.L. Chaboche: Plasticity, Mechanics of solid materials, Cambridge, UK (2000), 232-233.

[6] J.A. Nelder, R. Mead: A simplex method for function minimization, The computer Journal, 7 (1965), 308-313.

[7] R. Pérez, J. Benito, J. Prado: Study of the inelastic response of TRIP steels after plastic deformation. ISIJ International, 45 (2005), 152-158.